Hindawi
Journal of Cardiac Surgery
Volume 2023, Article ID 8872518, 8 pages
https://doi.org/10.1155/2023/8872518

Research Article

Cardiac Computed Tomography Assessment of the Variation of Papillary Muscle Morphology before Mitral Valve Surgery

Kenta Nishiya,[1] Yosuke Takahashi,[1] Keiichi Itatani,[2] Akimasa Morisaki,[1] Yoshito Sakon,[1] Goki Inno,[1] Yosuke Sumii,[1] Yukihiro Nishimoto,[1] Kazuki Noda,[1] Masataro Doi,[1] Munehide Nagao,[1] and Toshihiko Shibata[1]

[1]*Department of Cardiovascular Surgery, Osaka Metropolitan University Graduate School of Medicine, Osaka, Japan*
[2]*Department of Cardiovascular Surgery, Nagoya City University, Nagoya, Japan*

Correspondence should be addressed to Yosuke Takahashi; takahashi.yosuke@omu.ac.jp

Received 24 June 2023; Revised 18 September 2023; Accepted 13 December 2023; Published 29 December 2023

Academic Editor: Christopher Lau

Background. The morphology of the papillary muscles of the left ventricle is highly variable. Few studies have investigated papillary muscle morphology using imaging. *Objective*. This study aimed to assess papillary muscle morphology with primary mitral regurgitation (MR) using cardiac computed tomography (CT). *Methods*. We examined 116 patients who underwent robotic mitral valve repair for primary MR using preoperative cardiac CT. Papillary muscle morphology was assessed using CT images and compared with operative findings. *Results*. CT images of papillary muscles were consistent with the operative findings during robotic mitral valve repair in all cases. Both the anterolateral papillary muscle (APM) and posteromedial papillary muscle (PPM) groups were identified in all cases, and the middle papillary muscle (MPM) group was identified in 24.1% of cases. The PPM group had a higher proportion of complex morphologies with more heads and bases than the APM group (head: $p < 0.001$ and base: $p < 0.001$). The PPM group had smaller papillary muscle sizes than the APM group. The MPM group in most patients had one base and one head (78.6%). Papillary muscle sizes were significantly smaller in the order of the APM, PPM, and MPM groups ($p < 0.001$). *Conclusions*. Cardiac CT allowed clear visualization and accurate assessment of papillary muscle morphology in the left ventricle. It may be useful to obtain the papillary muscle variations preoperatively using CT imaging in procedures involving the papillary muscles such as mitral valve repair.

1. Introduction

The papillary muscles are one of the components of the mitral valve and typically consist of two papillary muscle groups, the anterior papillary muscle group and the posterior papillary muscle group, with various morphological diversities. Several previous studies have reported the morphological evaluation of papillary muscles in donated hearts [1–9]. However, these studies were conducted on normal hearts, and hearts with diseases, such as mitral regurgitation (MR), have rarely been investigated. In these previous studies, various classification methods for papillary muscle morphology based on its shapes can be found [2–6, 8]. However, it would be more clinically valuable to assess papillary muscle morphology in patients with cardiac diseases than to classify papillary muscle morphology in the normal heart.

Few studies have investigated papillary muscle morphology using imaging. One study used computed tomography (CT) imaging to assess papillary muscle morphology, mitral valve leaflet angle, and annulus size; however, this study focused on normal hearts and functional MR cases [10]. A review used magnetic resonance imaging (MRI) to assess papillary muscles, but it reported abnormalities of the papillary muscle itself, such as left ventricular outflow tract obstruction due to hypertrophy or malposition of the papillary muscle, congenital abnormalities of the parachute mitral valve, and ischemia or rupture of the papillary muscle, and did not cover primary MR [11]. In addition, these reports are based only on the assessment of images and have not compared these with actual gross findings, which do not ensure accuracy. Surgical procedures involving papillary muscles, such as artificial chordal replacement for mitral

valve prolapse and papillary muscle approximation for functional MR, have been widely performed. Although it is desirable to evaluate papillary muscles preoperatively, there is no established method to assess them preoperatively.

In the present study, we assessed the morphology of the papillary muscles using preoperative cardiac CT images in primary MR cases and evaluated the accuracy of the preoperative CT images by comparing them with the operative findings in robotic surgery. We also analyzed the positional distribution and size of the papillary muscles using CT images.

2. Materials and Methods

2.1. Study Population. Between October 2018 and July 2022, 120 patients underwent ECG-gated enhanced cardiac CT before robotic mitral valve repair. We excluded 4 cases due to etiology of MR: atrial functional MR ($n = 2$), ventricular functional MR ($n = 1$), and rheumatic MR ($n = 1$). In total, 116 patients who underwent robotic mitral valve repair for primary MR were included in this study.

2.2. Computed Tomography Scan and Analysis Protocol. A 320-row CT detector (Aquilion ONE/GENESIS Edition, Canon Medical Systems, Otawara, Japan) was used, following intravenous injection of 35–90 ml of nonionic contrast, the dose of which depended on body weight. The CT scan parameters were as follows: 320 rows × 0.5 mm; rotation time, 0.275 s; volume scan; tube voltage, 120 kV; and tube current, 800–1000 mAs. These methods were the same as in the previous study [12]. Multiphase images were reconstructed in 105 patients at every 10% of the cardiac cycle (0%–90%) as measured from one R wave to the next at a slice thickness of 0.5 mm and a slice interval of 0.5 mm.

For the analysis of the mitral apparatus anatomy, we selected diastole images (70% of the R-R cycle in one patient, 80% in 98 patients, 90% in 4 patients, and 0% in 2 patients) that visualized the papillary muscle morphology most clearly to construct 3D image of papillary muscles. Because there were no image data for all cardiac cycles, the studies of the remaining 11 patients were reconstructed at mid-diastole (75% of the R-R cycle) at a slice thickness of 0.5 mm and a slice interval of 0.25 mm.

A commercially available medical image analysis workstation (Synapse Vincent; Fujifilm Medical, Tokyo, Japan) was used to analyze the scanned CT data. The papillary muscles were segmented and reconstructed as a 3D image with a light blue color based on the angioscopy mode in the software. The mitral annulus was detected and reconstructed in 3D images by manually plotting the hinge curve of the mitral leaflet. Both right and left fibrous trigones were pointed out at the edge of the aorto-mitral continuity.

2.3. CT Images and Operative Findings. All CT images and surgical video images were saved. The author (K.N.) and the primary surgeon of robotic surgery (Y.T.) postoperatively compared the papillary muscle morphology of CT images with that of surgical images, retrospectively.

2.4. Papillary Muscle Classification. We defined the "midplane" as the plane perpendicular to the line connecting trigone to trigone through the middle point of both trigones. Papillary muscles located on the anterolateral commissure side of the midplane were defined as the anterolateral papillary muscle (APM) group and those located on the posteromedial commissure side were defined as the posteromedial papillary muscle (PPM) group. Papillary muscles crossing the midplane were defined as the middle papillary muscle (MPM) group (Figure 1). The papillary muscles from which the basal chordae originated were excluded from evaluation as basal papillary muscles.

The morphology of the papillary muscles was classified by the number of heads and bases, according to a method modified from a previous study [3]. When the papillary muscle had two or more heads on one base, the heads of the papillary muscle were defined as those with a height greater than 5 mm. For example, the present classification noted that the papillary muscle which had one head and one base was defined as H1B1 and that which had two heads and two bases was defined as H2B2 (Figure 2).

Several examples of comparisons between the CT images and surgical findings are shown in Figures 3(A)–3(D).

2.5. Papillary Muscle Measurement of Position and Size. To evaluate the positions of the papillary muscles, a Cartesian coordinate system was used, the origin of which was located at the middle of both trigones. The X-axis coincided with the line through both trigones. The Y-axis was defined as the line perpendicular to the X-axis that passed from the midpoint of both trigones to the hinge point of posterior mitral annulus. The coordinates of the apex of each papillary muscle head on the XY plane were measured manually (Figure 4(a)). The distance between the apex of each papillary muscle and the mitral annular plane (XY plane containing origin) is not measured in this study.

The sizes of the papillary muscle were measured as follows. Papillary muscle roots attach to the trabeculae carneae, which resemble the roots of a tree [13, 14]; these portions were not included in the measurements. The line connecting the point of the papillary muscle base closest to the left ventricle apex and the point of that closest to the mitral annulus was defined as the "baseline." The height of the individual papillary muscle from the lowest point of the baseline to the apex of the head was defined as the "major height." The height of the individual papillary muscle from the highest point of the baseline to the apex of the head was defined as the "minor height." In the plane parallel to the XY plane and containing the highest point of the baseline, the long diameter was defined as the "width" and the short diameter was defined as the "thickness" (Figure 4(b)).

All image creation and measurements were performed by a cardiac surgeon (K.N.), after which two other cardiac surgeons (Y.S. and G.I.) independently reassessed the accuracy of the measurements.

2.6. Ethical Statement. This study was approved by the Ethics Committee of Osaka Metropolitan University Graduate School of Medicine (approval number: 2020-066).

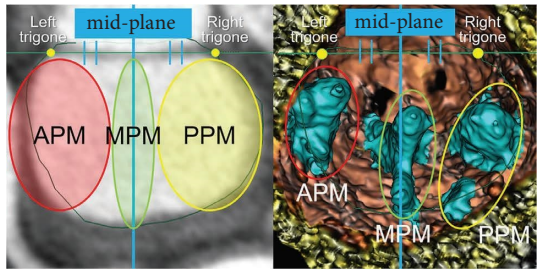

Figure 1: Classification of papillary muscle groups. The midplane is defined as the plane perpendicular to the line connecting the trigone to the trigone through the midpoint of both trigones. The APM group is defined as the papillary muscles located on the left trigone side of the midplane. The PPM group is defined as the papillary muscles located on the right trigone side of the midplane. The MPM group is defined as the papillary muscles crossing the midplane. APM, anterolateral papillary muscle; MPM, middle papillary muscle; and PPM, posteromedial papillary muscle.

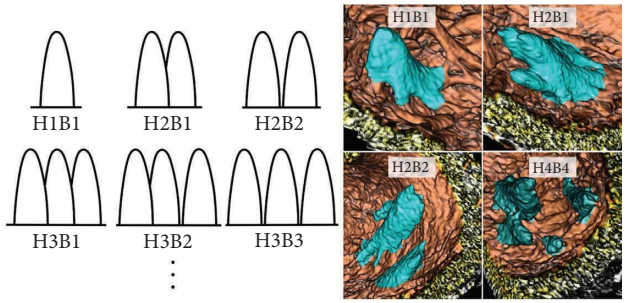

Figure 2: Morphological classification of papillary muscles. The papillary muscle morphology was classified according to the number of heads and bases. H1B1: Simple single muscle. H2B1: The origins of two head are common. H2B2: The two heads have their own origins. The same method was used when the numbers of heads and bases increased.

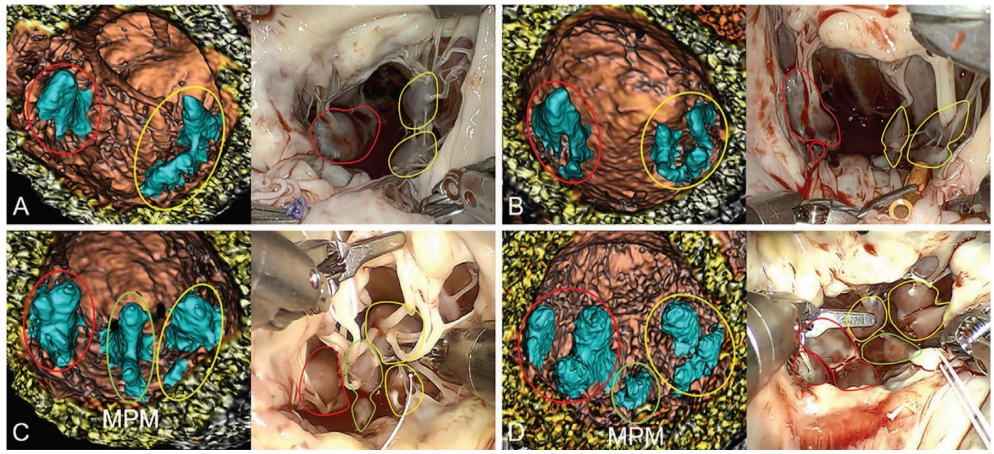

Figure 3: (A–D) Sample cases of comparison of CT images with operative findings. (A) The APM group has one head and one base (type H1B1) and the PPM group has two heads and two bases (type H2B2). (B) The APM group has one large head and one small head (type H2B2) and the PPM group has four small heads and two bases (type H4B2). (C) The APM group is type H1B1 and the PPM group is type H2B2. The MPM group has two heads and one base (type H2B1). (D) The APM group and PPM groups are type H3B2 and the MPM group is type H1B1. A total of seven heads are shown. APM, anterolateral papillary muscle; MPM, middle papillary muscle; and PPM, posteromedial papillary muscle.

2.7. Statistical Analysis. Data are presented as mean values ± standard deviation (SD) or median with interquartile range (IQR) as appropriate. Categorical variables are reported as percentages (%).

The Wilcoxon signed-rank test was used to compare the number of heads and bases between the APM and PPM groups. For comparisons among the three groups, one-way analysis of variance or the Kruskal–Wallis test was performed

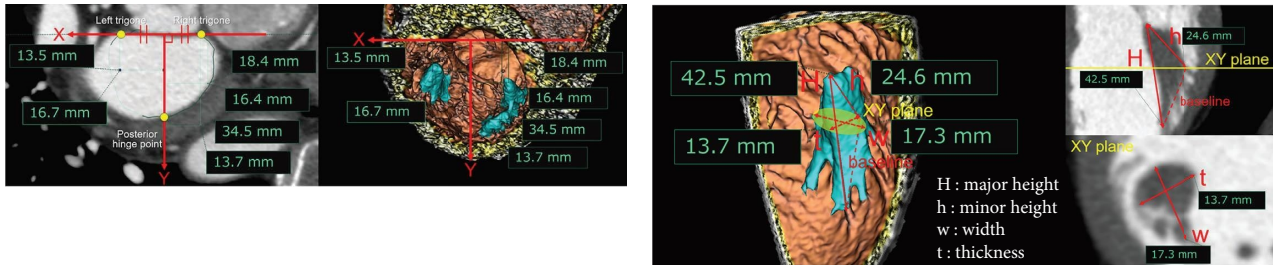

(a) (b)

Figure 4: Papillary muscle measurement. (a) Measurement of papillary muscle heads position assessed by the coordinate system. (b) Measurement of papillary muscle size.

after evaluating homoscedasticity using Bartlett's test. When a significant difference was observed among all the groups, the difference between each group was evaluated using the Bonferroni test. Correlation coefficients were calculated to measure the statistical dependence between the measured parameters. All statistical analyses were performed using EZR (Saitama Medical Center, Jichi Medical University, Saitama, Japan). A p value of less than 0.05 was considered statistically significant.

3. Results

3.1. Patient Population. A total of 116 patients (mean age of 60 ± 13 years, 68.1% male) were studied. There were two types of degenerative MR, including fibroelastic deficiency in 101 patients (87.1%) and Barlow's disease in 15 patients (12.9%). Patient characteristics are shown in Table 1.

3.2. CT Images and Operative Findings. The 3D images of the papillary muscles constructed from CT data were consistent with the operative findings of papillary muscle morphology in all cases.

3.3. Papillary Muscle Morphological Classification. Both the APM and PPM groups were identified in all cases. The MPM group was identified in 28 of 116 cases (24.1%). The morphological classification results for the papillary muscles are summarized in Table 2. The APM group had one head in 31.0%, two heads in 42.2%, three or more heads in 26.8%, one base in 54.3%, two bases in 33.6%, and three or more bases in 12.1% of the patients. The PPM group had one head in 12.9%, two heads in 34.5%, three or more heads in 52.6%, one base in 28.4%, two bases in 37.9%, and three or more bases in 33.7% of the patients. The PPM group had significantly more heads and bases than the APM group (head, $p < 0.001$; base, $p < 0.001$).

Most patients in the MPM group had a single base with one head (type H1B1, $n = 22$ (78.6%)). Intraoperative findings showed that most tendinous cords originating from the head in the MPM group were attached to P2 alone (74.3%), and 14.3% were attached to A2 (Table 3).

Table 1: Patient characteristics.

Patient characteristics	$n = 116$
Age (years), mean ± SD	60 ± 13
Male (%)	79 (68.1)
BSA (m^2), mean ± SD	1.69 ± 0.18
Etiology of MR	
Fibroelastic deficiency (%)	101 (87.1)
Barlow's disease (%)	15 (12.9)
Prolapse region of mitral valve	
Anterior leaflet (%)	16 (13.8)
Posterior leaflet (%)	74 (63.8)
Both leaflet (%)	22 (19.0)
Commissural leaflet (%)	4 (3.4)
Transthoracic echocardiography	
LVDd (mm), mean ± SD	53 ± 7
LVDs (mm), mean ± SD	31 ± 6
LVEF (%), mean ± SD	62 ± 5
MR (over moderate) (%)	100 (100)
TR (over moderate) (%)	6 (5.2)

BSA, body surface area; LVEF, left ventricular ejection fraction; LVDd, left ventricular diastolic dimension; LVDs, left ventricular systolic dimension; MR, mitral regurgitation; SD, standard deviation; TR, tricuspid regurgitation.

3.4. Papillary Muscle Measurement of Position and Size. A scatter plot of the apex position of each papillary muscle head is shown in Figure 5. The difference in the size of each point represents the relative difference in the major heights of each papillary muscle. The mean coordinates of the apex position were 13.9 ± 4.6, 18.9 ± 8.3 in the APM group; -16.5 ± 5.4, 24.8 ± 9.6 in the PPM group; and 0.8 ± 2.6, 30.6 ± 8.7 in the MPM group. The MPM group was distributed around the Y-axis, most of which were within 5 mm of the Y-axis. Few papillary muscles were distributed around the left ventricular outflow tract.

The size measurements for each papillary muscle group are shown in Figure 6.

Significant differences were found in the mean of each size measurement among the three groups (major height, $p < 0.001$; minor height, $p < 0.001$; width, $p < 0.001$; and thickness, $p < 0.001$). All size measurements were significantly smaller in the order the APM, PPM, and MPM groups.

No significant correlation was found between the X coordinates of the papillary muscle apex and each size measurement in the APM, PPM, and MPM groups. The

Table 2: Morphological classification results of the papillary muscles.

APM $n = 116$	B1	B2	B3	B4	B5	B6	Total
H1	36 (31.0%)						36 (31.0%)
H2	25 (21.6%)	24 (20.7%)					49 (42.2%)
H3	2 (1.7%)	15 (12.9%)	8 (6.9%)				25 (21.6%)
H4	0	0	2 (1.7%)	3 (2.6%)			5 (4.3%)
H5	0	0	0	0	1 (0.9%)		1 (0.9%)
H6	0	0	0	0	0	0	0
Total	63 (54.3%)	39 (33.6%)	10 (8.6%)	3 (2.6%)	1 (0.9%)	0	116 (100%)
PPM $n = 116$	B1	B2	B3	B4	B5	B6	Total
H1	15 (12.9%)						15 (12.9%)
H2	13 (11.2%)	27 (23.3%)					40 (34.5%)
H3	5 (4.3%)	15 (12.9%)	25 (21.6%)				45 (38.8%)
H4	0	2 (1.7%)	4 (3.4%)	8 (6.9%)			14 (12.1%)
H5	0	0	0	1 (0.9%)	0		1 (0.9%)
H6	0	0	0	0	0	1 (0.9%)	1 (0.9%)
Total	33 (28.4%)	44 (37.9%)	29 (25.0%)	9 (7.8%)	0	1 (0.9%)	116 (100%)
MPM $n = 28$	B1	B2	B3	B4	B5	B6	Total
H1	22 (78.6%)						22 (78.6%)
H2	4 (14.3%)	1 (3.6%)					5 (17.9%)
H3	0	0	1 (3.6%)				1 (3.6%)
H4	0	0	0	0			0
H5	0	0	0	0	0		0
H6	0	0	0	0	0	0	0
Total	26 (92.9%)	1 (3.6%)	1 (3.6%)	0	0	0	28 (100%)

APM, anterolateral papillary muscle; MPM, middle papillary muscle; PPM, posteromedial papillary muscle.

Table 3: The assessment of the attachment site of tendinous cords extending from MPM heads by operative findings.

	n (%)
Total number of MPM heads	35 (100.0)
P2	26 (74.3)
A2	5 (14.3)
P2P3	2 (5.7)
P1P2	1 (2.9)
P3	1 (2.9)

minor height and thickness were correlated with Y coordinates in all papillary muscle groups: minor height (APM, $r = -0.283$ and $p < 0.001$; PPM, $r = -0.313$ and $p < 0.001$; and MPM, $r = -0.354$ and $p = 0.037$) and thickness (APM, $r = -0.219$ and $p < 0.001$; PPM, $r = -0.197$ and $p < 0.001$; and MPM, $r = -0.428$ and $p = 0.010$).

4. Discussion

Our study showed that (1) preoperative cardiac 4D CT used to assess the morphology of the papillary muscles of the left ventricle was consistent with the intraoperative findings and allowed clear visualization and accurate assessment of the papillary muscle morphology and (2) the middle papillary muscle group, which was located between the APM and PPM groups, was found in about a quarter of the cases in this study.

This study analyzed the distribution of each papillary muscle within the left ventricle and classified each papillary muscle into APM, PPM, and MPM groups. Robot-assisted surgery provides an excellent view of the whole papillary muscles, and we believe that the preoperative CT evaluation and the intraoperative evaluation may be reconciled with high accuracy. Although there are a few reports on MPM [15, 16], to our knowledge, this is the first report to define MPM. Papillary muscles are divided into APM and PPM groups during the embryonic period [15], and it is thought that MPM may arise as a variant of this developmental process.

The MPM group (mean major height: 20.2 ± 8.6 mm) was smaller in height than both the APM group (mean major height: 30.1 ± 9.4 mm) and the PPM group (mean major height: 26.0 ± 9.1 mm). Most of the chordae tendineae originating from the head of the MPM group were found to attach only to P2 of the mitral valve leaflet (74.3%), but 14.3% of the chordae tendineae attached to A2. Four of the 28 cases (14.3%) who had the MPM group in this study had an artificial chordal replacement in the body of the MPM group. The mean major height of the MPM heads used to anchor the artificial chordae was 29.5 mm, which was relatively high in others among the MPM group. Although the height of the MPM group was smaller than that of the APM and PMP groups, the middle papillary muscles may be used for artificial chordae reconstruction if the size of them is large enough.

In the present study, the PPM group had a higher proportion of complex morphology with more heads and bases than the APM group. These findings were consistent with those of previous studies [1–7]. The reason why MR prolapse is more common in the medial half may be due to the diversity of the posterior papillary muscles. Papillary muscles are formed during the embryonic stage due to delamination of the left ventricular musculature [15]. Therefore, the morphology of each papillary muscle group is very diverse, and it is no

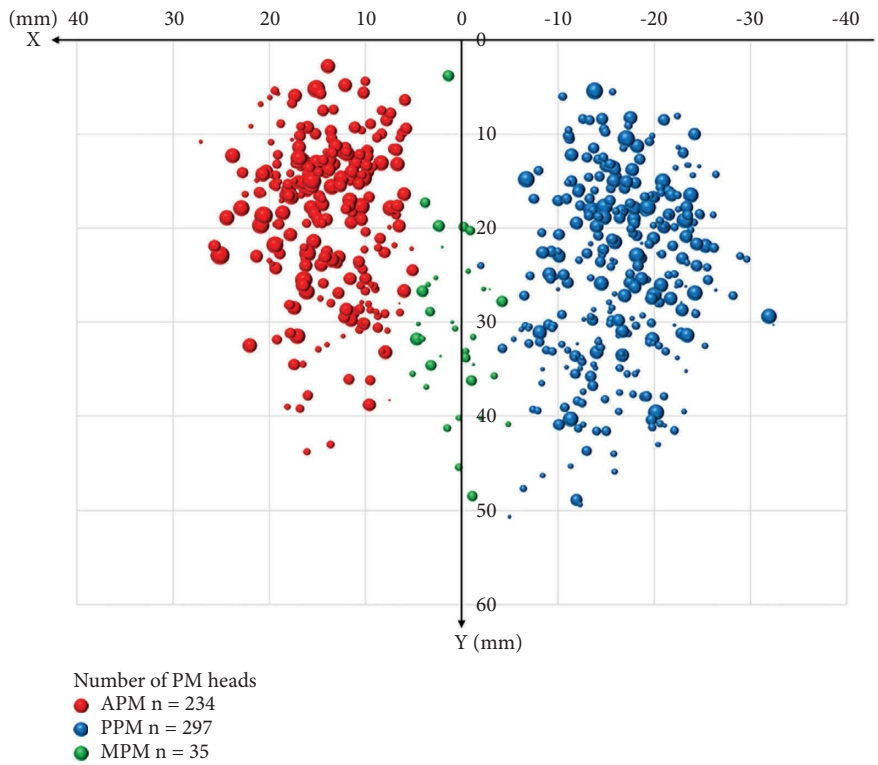

Figure 5: The scatter plot of the apex position of each papillary muscle head. The difference in the size of each point represents the relative difference in the major heights of each papillary muscle. APM, anterolateral papillary muscle; MPM, middle papillary muscle; and PPM, posteromedial papillary muscle.

exaggeration to say that none of the cases had the same papillary muscles morphology as an arbitrary case. In previous studies, various classification methods have been used to categorize papillary muscles morphology [2–6, 8]. In this study, the classification was based on the number of heads and bases of the papillary muscle. It is beneficial to be able to assess the morphology, positioning, and size of the papillary muscles in each MR case preoperatively. This study showed that such information could be obtained preoperatively using cardiac CT.

4.1. Surgical Implication. The gold standard for preoperative examination of mitral valve surgery is transesophageal echocardiography (TEE), which provides a detailed assessment of the prolapse site, leaflet mobility, and degree of regurgitation [17, 18]. In contrast, anatomical characterization of the relationship between the mitral valve annulus and the coronary artery can be assessed in detail using CT [12]. There are also a few studies on the morphological assessment of papillary muscles using imaging techniques such as CT and MRI [10, 11]. In the present study, cardiac 4D CT was used to image the structures of the papillary muscles at the appropriate cardiac phase, and 3D images were constructed for clear visualization.

In mitral valve repair, artificial chordae are sutured to the papillary muscle corresponding to the prolapsed valve leaflet [19]. However, the corresponding papillary muscle may sometimes be small and fragile, and artificial chordal reconstruction may need to be performed from other large papillary muscles [20]. Mitral valve repair with subvalvular apparatus intervention, such as approximation of the papillary muscle for ventricular functional mitral regurgitation, has also been performed [21, 22]. For these surgical procedures, it may be useful to clearly visualize the papillary muscle morphology in preoperative imaging studies, so that the papillary muscle for suturing the artificial chordae can be determined preoperatively.

4.2. Limitation. First, the participants in this study were all primary MR cases, and unlike other studies on papillary muscle morphology, they did not reflect the characteristics of all populations, including healthy subjects. Variations in papillary muscle morphology may play a role in susceptibility to mitral regurgitation, but this analysis should be conducted in the future. Second, papillary muscle position and size were measured during the diastolic phase, and we were not able to investigate these changes during the systolic phase. This is because it is difficult to image papillary muscle morphology accurately during the systolic phase. There is no dispute that it is during the systolic phase that regurgitation actually occurs in the mitral valve and that it would be desirable to know the anatomical position and function of the papillary muscles during the systolic phase.

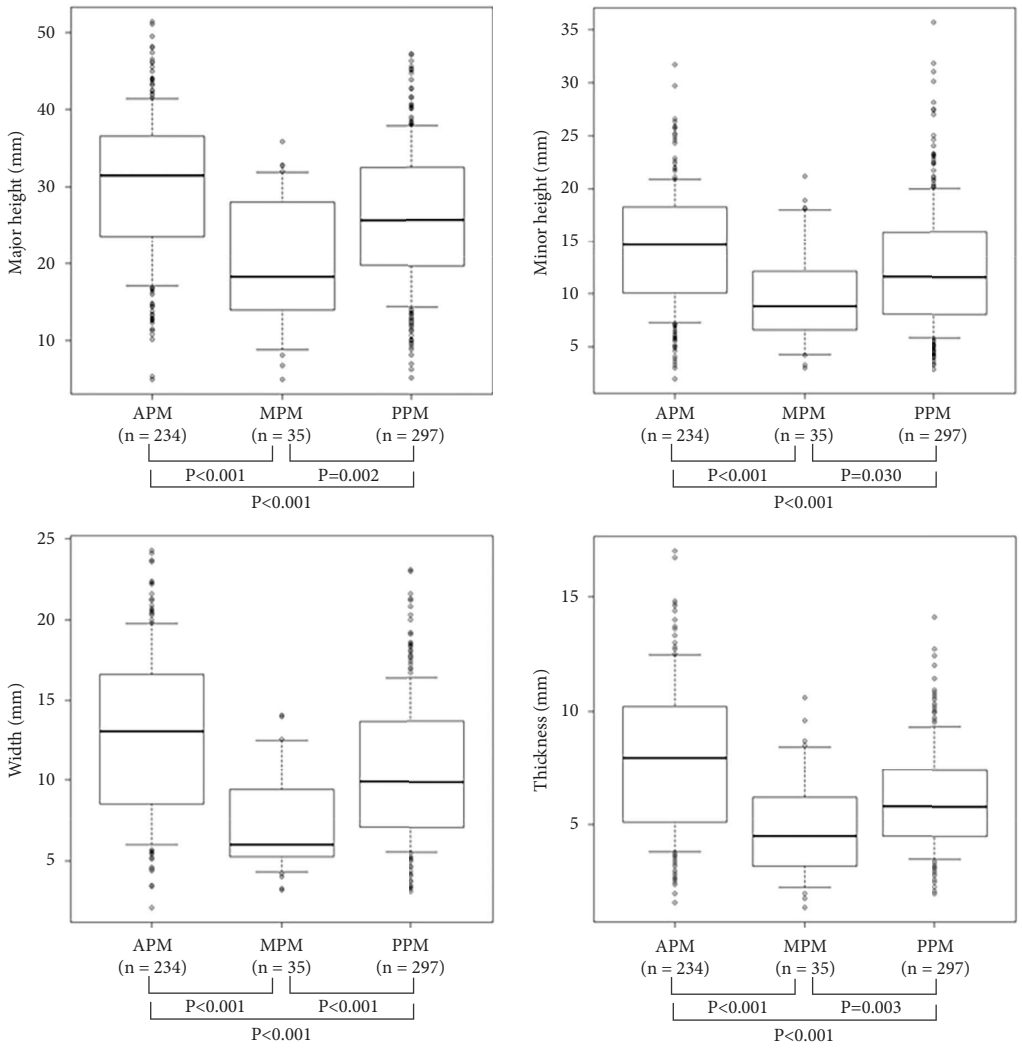

Figure 6: The sizes of each papillary muscle group.

5. Conclusion

In this study, cardiac CT allowed clear visualization and accurate assessment of the papillary muscle morphology of the left ventricle. The middle papillary muscle group, located between the APM and PPM groups, was found in approximately one-quarter of the cases in this study. It may be useful to obtain detailed preoperative information on the papillary muscles by using imaging studies in procedures involving the papillary muscles, such as artificial chordal replacement and papillary muscle approximation.

Data Availability

The data used in this study are available from the corresponding author upon request due to privacy/ethical restrictions.

Conflicts of Interest

The authors declare that they have no conflicts of interest regarding the publication of this paper.

References

[1] W. C. Roberts and L. S. Cohen, "Left ventricular papillary muscles: description of the normal and a survey of conditions causing them to be abnormal," *Circulation*, vol. 46, no. 1, pp. 138–154, 1972.

[2] S. Victor and V. M. Nayak, "Variations in the papillary muscles of the normal mitral valve and their surgical relevance," *Journal of Cardiac Surgery*, vol. 10, no. 5, pp. 597–607, 1995.

[3] D. Berdajs, P. Lajos, and M. I. Turina, "A new classification of the mitral papillary muscle," *Medical Science Monitor: International medical journal of experimental and clinical research*, vol. 11, no. 1, pp. 18–21, 2005.

[4] B. Shree, R. K. Singla, R. Sharma, and A. Kumar, "A study of papillary muscles of the left ventricle in the adult human cadavers," *International Journal of Anatomy and Research*, vol. 4, no. 2.2, pp. 2285–2293, 2016.

[5] A. Saha and S. Roy, "Papillary muscles of left ventricle-Morphological variations and it's clinical relevance," *Indian Heart Journal*, vol. 70, no. 6, pp. 894–900, 2018.

[6] S. Valli and G. Gohila, "Study of anatomical variations of mitral papillary muscles and their significance: a cadaveric

study from southern India," *International Journal of Anatomy Radiology & Surgery*, vol. 10, no. 4, pp. 30–33, 2021.

[7] A. Krawczyk-Ożóg, M. K. Hołda, F. Bolechała et al., "Anatomy of the mitral subvalvular apparatus," *The Journal of Thoracic and Cardiovascular Surgery*, vol. 155, no. 5, pp. 2002–2010, 2018.

[8] G. Sa, W. Rn, and F. Ms, "Morphological variations of papillary muscles in the mitral valve complex in human cadaveric hearts," *Singapore Medical Journal*, vol. 54, no. 1, pp. 44–48, 2013.

[9] M. B. Sinha, S. K. Somkuwar, D. Kumar, and D. K. Sharma, "Anatomical variations of papillary muscles in human cadaveric hearts of Chhattisgarh, India," *Indian Journal of Clinical Anatomy and Physiology*, vol. 7, no. 4, pp. 374–380, 2021.

[10] V. Delgado, L. F. Tops, J. D. Schuijf et al., "Assessment of mitral valve anatomy and geometry with multislice computed tomography," *JACC Cardiovascular Imaging*, vol. 2, no. 5, pp. 556–565, 2009.

[11] P. Rajiah, N. L. Fulton, and M. Bolen, "Magnetic resonance imaging of the papillary muscles of the left ventricle normal anatomy, variants, and abnormalities," *Insights into Imaging*, vol. 10, no. 1, p. 83, 2019.

[12] N. Kishimoto, Y. Takahashi, H. Fujii et al., "Computed tomography to identify risk factors for left circumflex artery injury during mitral surgery," *European Journal of Cardio-Thoracic Surgery*, vol. 61, no. 3, pp. 675–683, 2022.

[13] L. Axel, "Papillary muscles do not attach directly to the solid heart wall," *Circulation*, vol. 109, no. 25, pp. 3145–3148, 2004.

[14] M. S. Khan and R. Biederman, "Dynamic cardiac anatomy the "cypress tree" papillary muscle root," *Journal of Cardiovascular and Thoracic Research*, vol. 10, no. 3, pp. 138–143, 2018.

[15] P. W. Oosthoek, A. C. Wenink, L. J. Wisse, A. C. Gittenberger-de Groot, and G. Gittenberger-de, "Development of the papillary muscles of the mitral valve: morphogenetic background of parachute-like asymmetric mitral valves and other mitral valve anomalies," *The Journal of Thoracic and Cardiovascular Surgery*, vol. 116, no. 1, pp. 36–46, 1998.

[16] A. Carpentier, D. H. Adams, and F. Filsoufi, *Carpentier's Reconstructive Valve Surgery*, Saunders, PA, USA, 2010.

[17] C. M. Otto, R. A. Nishimura, R. O. Bonow et al., "2020 ACC/AHA guideline for the management of patients with Valvular Heart disease: a report of the American college of cardiology/American heart association joint committee on clinical practice guidelines," *Journal of the American College of Cardiology*, vol. 77, no. 4, pp. e25–e197, 2021.

[18] A. Vahanian, F. Beyersdorf, F. Praz et al., "2021 ESC/EACTS Guidelines for the management of valvular heart disease," *European Heart Journal*, vol. 43, no. 7, pp. 561–632, 2022.

[19] T. E. David, J. Bos, and H. Rakowski, "Mitral valve repair by replacement of chordae tendineae with polytetrafluoroethylene sutures," *The Journal of Thoracic and Cardiovascular Surgery*, vol. 101, no. 3, pp. 495–501, 1991.

[20] T. Shibata, "Loop technique for mitral valve repair," *General Thoracic and Cardiovascular Surgery*, vol. 62, no. 2, pp. 71–77, 2014.

[21] A. Rama, L. Praschker, E. Barreda, and I. Gandjbakhch, "Papillary muscle approximation for functional ischemic mitral regurgitation," *The Annals of Thoracic Surgery*, vol. 84, no. 6, pp. 2130-2131, 2007.

[22] S. Wakasa, S. Kubota, Y. Shingu, T. Ooka, T. Tachibana, and Y. Matsui, "The extent of papillary muscle approximation affects mortality and durability of mitral valve repair for ischemic mitral regurgitation," *Journal of Cardiothoracic Surgery*, vol. 9, no. 1, pp. 98–106, 2014.